Technical journals online.com

Research Paper

ENHANCED POWER EFFICIENT ANTENNA SWITCHING (EPEAS) FOR QOS IMPROVEMENT OF LTE DOWNLINK

*MUGELAN.R.K, +CHANTHIRASEKARAN.K, *BHAGYAVENI.M.A

Address for Correspondence

*,+Department of Electronics and Communication Engineering,
*College of Engineering Guindy, +Anand Institute of Higher Technology
Anna University, Chennai, Tamil Nadu, India.

ABSTRACT

Long Term Evolution (LTE) is the next major step in mobile communications.. Multiple input multiple output (MIMO) technique, is a key technology to achieve the peak data rates, low latency and spectral efficiency targets of LTE systems. The Quality of Service (QoS) of the MIMO system degrades in a highly correlated channel. The aim of the proposed work is to provide guaranteed QoS with optimal power under highly correlated channel conditions. To achieve the above objective, Enhanced Power Efficient Antenna Switching (EPEAS) strategy is proposed. This technique employs adaptive antenna switching between SISO/SIMO/MISO/MIMO modes based on channel characteristics. By adaptively switching to other modes from MIMO one transmitter or receiver or both transceiver chains are powered off thus reducing the power consumption as well as reducing the channel correlation. In addition to switching, a novel Error Vector Magnitude (EVM) based Constellation Combiner (ECC) is employed, which picks up the most optimal signal constellation for decoding from the received multipath signals thereby improving the performance. The proposed algorithm is evaluated in real time indoor channel using Wireless Open Access research Platform (WARP) test bed. The results prove that EPEAS achieves an improvement of 22.3% than the conventional MIMO mode of transmission.

KEYWORDS: SISO, SIMO, MISO, MIMO, ECC, EVM, Antenna Switching, Wireless Open Access Research Platform, LTE.

1. INTODUCTION

LTE is the next major step in mobile communication major requirements for the current worldwide scenario are high speed data rate, higher spectral efficiency, improved services and lower latency as well as high-capacity voice support.LTE primarily uses the concept of MIMO and OFDM. Multiple input multiple output (MIMO) technique that requires multiple antennas at both transmitter and receiver is a key technology to meet the targets of LTE. Although MIMO can improve system transmission rate it is unable to demodulate the signal and may produce data loss when the channel has stronger correlation [1]. A possible solution for the above problem is to switch between the modes of antenna MIMO/MISO/SIMO/SISO in order to maintain the promised QoS. In particular, the proposed solution not only offers guaranteed QoS to the mobile user, but it also achieves this through efficient power management techniques. As it has been pointed out in [2], the radio access part of the wireless network accounts for up to more than 70% of the total energy bill for a number of mobile operators. Therefore, developing energy-efficient wireless architectures and technologies is crucial to meet this challenge.

In [3], the authors discuss about MIMO mode adaptation schemes based on channel correlation, Rank, Doppler shift and SNR. It has high computation complexity and does not consider any power saving methods. In [4] the adaptive MIMO mode switching in LTE downlink system based on SINR and channel correlation (CSI) was discussed. The technique achieved higher reliability, but energy efficiency was not analyzed. In [5] the authors has discussed about antenna switching in LTE cellular networks based on different traffic load conditions by turning off one of the MIMO antennas to make the system energy efficient. But the energy efficiency is achieved in terms of QoS degradation of real time traffic sources.The error performance of BPSK-modulated distributed selection combining (SC) and distributed switched-and-stay combining (DSSC) are studied in [6]. It makes use of lower order modulation and linear combining. The literature [7] describes the performance improvement using EGC with no CSI. The combining technique used at the destination is complex compared to ECC. In [8] the authors discuss the performance using PSK and QAM modulation with MRC, which have high complexity and thereby increase the power consumption.

In this paper, we analyze performance of MIMO, MISO, SIMO and SISO for various transmitting power using WARP test bed based on BER, EVM and SNR. Using above results a decision block has been designed with which the adaptive switching is done. EVM is calculated from the received signal constellation diagram which is used to assess the quality of digitally modulated signal [9]. The proposed work has been done in wireless research test bed called wireless open access research platform (WARP).WARP provides a scalable and configurable platform to prototype wireless communication algorithms for educational and research oriented applications.

The rest of the paper is organized as follows. Section II provides an introduction to system modules for EPEAS model. Section III outlines the motivation for the proposed work. The real-time evaluation of EPEAS strategy is analyzed in Section IV followed by power saving calculation in section V. Conclusion is stated in Section VI.

2. INTRODUCTION TO SYSTEM MODULES FOR EPEAS

In this section, brief introductions to various modules that are used for the implementation and evaluation of EPEAS strategy have been discussed.

2.1 *Wireless Open Access Research Platform*

The WARP platform shown in Fig.2.1 was designed at Rice University and is used in a number of academic and industrial research laboratories for clean state protocol implementation of the MAC and PHY [10]. A WARPV3 kit usually contains two RF radio boards (RF-A, RF-B) which is suitable for SISO transmission, each RF board can be configured as either transmitter or receiver. Two more RF boards (RF-C, RF-D) can be added via FMC (FPGA Mezzanine Connector) for MIMO transmission.

MIMO capable radios operate in 2.4/5GHz frequency ranges and can support wideband applications.

The algorithm that has to be tested using WARP test bed will be written using WARPLAB interface commands which enable the WARP board to act as the designed module. The board is initialized using '.bit' file using WARPLAB reference design using a JTAG cable or SD card. Once these procedures are completed, the test bed is now fully operational. By transmitting and receiving the signals using the WARP board the EPEAS results are evaluated.

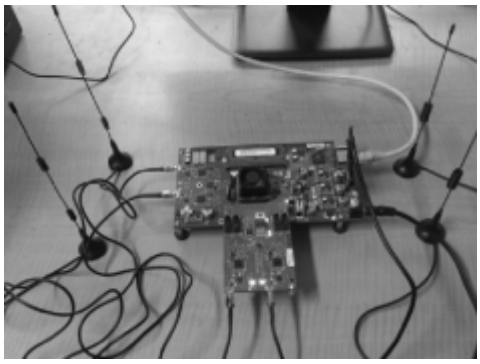

Figure 2.1 Experimental setup of WARP

2.2*WARPLab*

WARPLab is a framework for rapid prototyping that allows coordination of arbitrary combination of single and multi-antenna transmit and receive nodes. The extensible framework gives the user flexibility to develop and deploy large array of nodes to meet any application or research need. WARPLab reference design is an implementation of the WARPLab framework that allows many physical layer designs to be constructed and tested. The reference design combines MATLAB and FPGA implementations of WARPLab framework modules that allow for easy extensibility and customization. While reference design uses MATLAB to control nodes and perform signal processing, it also allows application with strict latency requirements to move time critical processing in to FPGA.

2.3 *QoS enhancement module at the Transmitter end (Alamouti scheme)*

Alamouti scheme is one among the several space-time diversity techniques that can be used in 2x1 MISO mode or in a 2x2 MIMO mode. The Alamouti block code is the only complex block code that has a data rate of 1 while achieving maximum diversity gain.

Here a single data stream is divided in two and fed to two transmitting antennas. Consider that two symbols $s_1$and s_2 are transmitted simultaneously from transmit antennas 1 and 2 during the first symbol period, while symbols$-s_2^*$ and s_1^* are transmitted from antennas 1 and 2 during the next symbol period. Here the Alamouti scheme is executed using WARP test bed in an indoor environment. It has been found that the channel is observed to be a flat fading channel with Line Of Sight (LOS) and it remains constant over the two successive symbol periods. The 2×2 channel matrix reads as (1), the values of the channel coefficients in (1) are found using preamble and Long Training Sequences (LTS). The values tend to change over a period of time based on the channel condition.

$$H = \begin{bmatrix} h_{11} & h_{12} \\ h_{21} & h_{22} \end{bmatrix} \quad (1)$$

The vector signal received at the receive array at the first symbol period is given by (2),

$$r_1 = \sqrt{E_s} H \begin{bmatrix} s_1/\sqrt{2} \\ s_2/\sqrt{2} \end{bmatrix} + n_1 \quad (2)$$

And the vector signal received at the second symbol period is given by (3)

$$r_2 = \sqrt{E_s} H \begin{bmatrix} -s_2^*/\sqrt{2} \\ s_1^*/\sqrt{2} \end{bmatrix} + n_1 \quad (3)$$

Where n_1 and n_2 are the additive noise contributions at each symbol period over the receive antenna array. The receiver forms a combined signal vector 'y' described mathematically in (4),

$$r = \begin{bmatrix} r_1 \\ r_2^* \end{bmatrix} = \sqrt{E_s} \underbrace{\begin{bmatrix} h_{11} & h_{12} \\ h_{21} & h_{22} \\ h_{12}^* & -h_{11}^* \\ h_{22}^* & -h_{21}^* \end{bmatrix}}_{H_{eff}} \underbrace{\begin{bmatrix} s_1/\sqrt{2} \\ s_2/\sqrt{2} \end{bmatrix}}_{s} + \begin{bmatrix} n_1 \\ n_2^* \end{bmatrix} \quad (4)$$

Both symbols s_1 and s_2 are spread over the two transmit antennas and over the two symbol periods. Furthermore, H_{eff} is orthogonal for all channel realizations i.e., $H_{eff}^H H_{eff} = \|H\|_F^2 I_2$ .After computing$z = H_{eff}^H r$ (5), we get

$$z = \begin{bmatrix} z_1 \\ z_2 \end{bmatrix} = \sqrt{E_s} H_{eff}^H r = \|H\|_F^2 I_2 s + n' \quad (5)$$

Wheren' is such that

$\varepsilon\{n'\} = 0_{2x1}$and $\varepsilon\{n'n'^H\} = \|H\|_F^2 \sigma_n^2 I_2$.

The above equation illustrates that the transmission of s_1 and s_2 is fully decoupled [9]. In general equation (5) is re-written as (6)

$$z_k = \sqrt{E_s/2}\, \|H\|_F^2 s_k + \widehat{n_k} \quad (k=1, 2) \quad (6)$$

2.4 *QoS enhancement module at the receiver end - Error Vector Magnitude (EVM) based Constellation Combiner (ECC)*

Diversity combining techniques are the widely employed technique to combine the data from multiple paths. Some prominent techniques include Selection combining, threshold combining, Equal Gain Combining (EGC) and Maximal Ratio Combining (MRC). First two techniques are linear combining which are less efficient than EGC and MRC. One major drawback of EGC and MRC is the computation complexity which increases the energy consumption. So in order to reduce the computational energy requirement a diversity combining technique called ECC is being used here.

After receiving the symbols, error vector magnitude is found to assess the quality of the received signal. Error Vector Magnitude is the vector difference between transmitted signal (ideal symbol) and received signal (measured symbol). EVM helps in identifying sources of signal degradation i.e., phase noise, I-Q imbalance, amplitude non-linearity and filter distortion. Error Vector Magnitude [11] is mathematically expressed as (7) and (8).

$$EVM = \sqrt{\frac{\frac{1}{N}\sum_{K=1}^{N}(e_K)}{\frac{1}{N}\sum_{K=1}^{N}(I_K^2 + Q_K^2)}} \quad (7)$$

$$e_K = (I_K - \widetilde{I_k})^2 + (Q_K - \widetilde{Q_k})^2 \quad (8)$$

Where I_k and Q_k are ideal values (transmitted symbols) and $\widetilde{I_k}$ and $\widetilde{Q_k}$ are received symbols I_k is the inphase measurement of the k^{th} symbol in the burst, Q_k is the Quadrature phase measurement of the k^{th} symbol in the burst and N is the input vector length

The EVM is calculated for the symbols that are received in antenna 1 and in antenna 2. The minimum of the Euclidian distance is calculated for each symbol received in both the antennasand a new version of the constellation is obtained with an optimal EVM as shown in Fig 2.2

ECC can be mathematically depicted as described in [12] equation (9) and (10)

$$EVM_{ECC} = \sqrt{\frac{\frac{1}{N}\sum_{K=1}^{N}(e_{ECC})}{\frac{1}{N}\sum_{K=1}^{N}(I_K{}^2+Q_K{}^2)}} \quad (9)$$

$$e_{ECC} = \min[(I_K - I_K^a)^2 + (Q_K - Q_K^a)^2, (I_K - I_K^b)^2 + (Q_K - Q_K^b)^2] \quad (10)$$

Where, I_K^a and Q_K^a are the inphase and quadrature phase symbols drawn from the received data at antenna-1. I_K^b and Q_K^b are the Inphase and Quadrature phase symbols drawn from the received data at antenna-2.

The Fig. 2.3 shows the performance evaluation of ECC for various transmit powers, it can be seen that the proposed combiner gives a better performance by reducing the BER. It is evident that ECC achieves gives a BER performance improvement of 24.42% in comparison than the BER of data from both antenna 1 and 2.

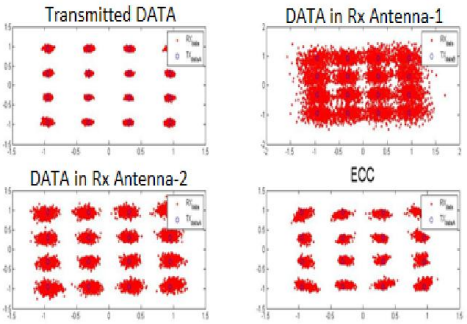

Figure 2.2 Effect of ECC

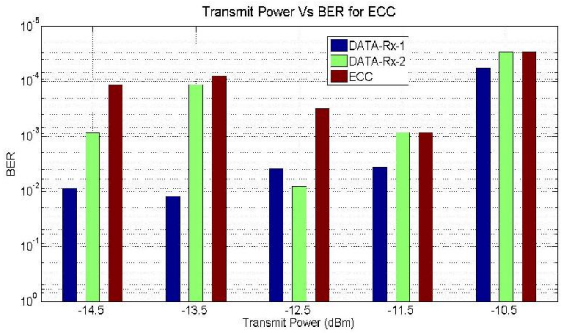

Fig. 2.3 Performance Evaluation of ECC

3. MOTIVATION

3.1 *MIMO performance*

Initially the performance of a MIMO mode of transmission has been evaluated for the experimental parameters as given in Table I. It is observed from Fig 3.1 that there is a performance degradation resulting in degraded QoS after a certain level of transmission power. For experimentally evaluating the proposed EPEAS strategy the range of Transmit power level has been chosen between -21.5 dBm to -7 dBm. The performance of MIMO has been evaluated in the chosen power levels, Fig.3.1 shows the BER performance of MIMO mode by increasing the transmit power between -21.5 dBm to -7 dBm while keeping the receiver baseband gain at 29.5 dB. From a transmit power level of -18.5dBm to -11.5dBm a QoS of $>10^{-6}$which is about 44% of the entire power level is considered.

Table I: Experimental Parameters

Parameters	Values
Number of bits	32768
Number of OFDM Symbols	180
Modulation Order	16(16-QAM)
Transmitter RF gain mode[13]	High
Transmitter Power (dBm) [13]	-24.5 to -7.0005
Receiver LNA gain[13]	40 dB
Receiver BB gain[13]	29.5
MIMO mode	2x2
Transmitter-Receiver Distance	1.5 m

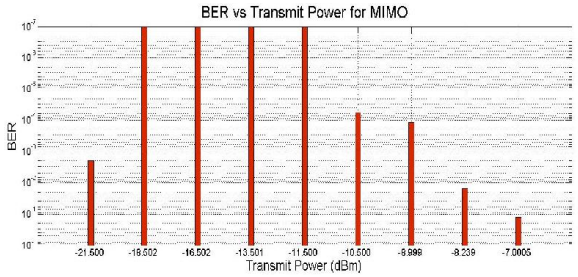

Fig. 3.1 Performance Evaluation of MIMO

In order to increase the guaranteed QoS of the MIMO system in the chosen range of power level, EPEAS strategy is proposed.

4. ENHANCED POWER EFFICIENT ANTENNA SWITCHING (EPEAS) STRATEGY MODEL

In this section the detailed flow of the EPEAS transceiver chain implemented in WARP test bed has been explained. The proposed strategy model has two phases namely Decision Phase and Transmitting Phase.

4.1 *Decision Phase*

This phase is the initializing part of the EPEAS strategy model, where the transmission of a known data sequence is done using all four modes MIMO/MISO/SIMO/SISO. From the received signals the BER and EVM% are obtained as shown in Fig. 4.1 (a) and (b).

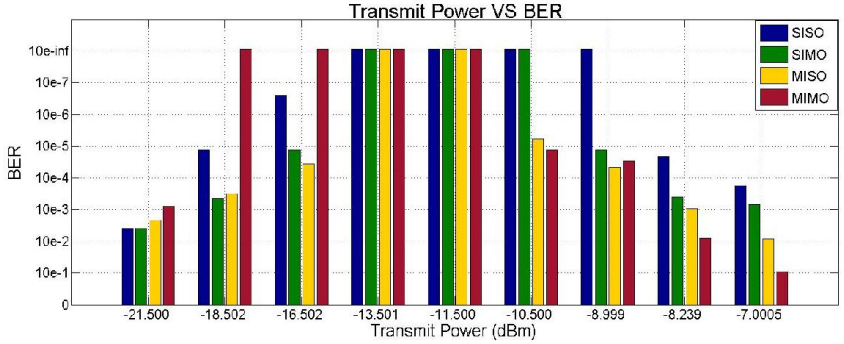

(a)

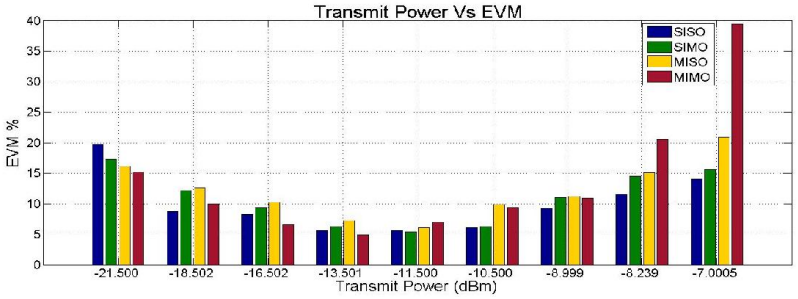

(b)

Fig 4.1 Performance metrics with varying Transmit Power

From the above results the EPEAS decision block for switching between various modes is formulated by fixing the operating points for each mode as described by values given in Table II-V to achieve the required BER of less than 10^{-6}.

Table II: Operating Point of MIMO

BER<10^{-6}; EVM < 10%; Rx_BB_Gain = 29.5 dB		
P_t (dBm)	EVM%	SNR (dB)
-18.502	9.97	20.02
-16.502	6.57s	23.52

Table III: Operating Point of MISO

BER<10^{-6}; EVM < 10%; Rx_BB_Gain = 29.5 dB		
P_t (dBm)	EVM%	SNR (dB)
-13.500	7.306	22.73

Table IV: Operating Point of SIMO

BER<10^{-6}; EVM < 10%; Rx_BB_Gain = 29.5 dB		
P_t (dBm)	EVM%	SNR (dB)
-11.500	5.417	25.325

Table V: Operating Point of SISO

BER<10^{-6}; EVM < 10%; Rx_BB_Gain = 29.5 dB		
P_t (dBm)	EVM%	SNR (dB)
-10.500	6.164	24.20
-8.99	9.318	20.61

It can be seen from Fig. 4.1 and Tables II, III, IV and V that the transmit power range of -18.5dBm to -16.5dBm MIMO mode achieves the required QoS of BER<10^{-6}. If the transmit power is -13.502 dBm, the performance of MIMO mode is poor because of the correlated channel which is evident from Fig. 4.1. So the mode of operation is switched to MISO. This is achieved by switching off one receiver chain and reducing the ill effects of the channel to provide the desired BER. Though MIMO, MISO, SIMO and SISO gives desired QoS for the transmit power levels -13.500 dBm and -11.502 dBm, it can be seen that MISO achieves the required BER with low SNR at -13.500 dBm. Similarly when there is a further increase of power to the maximum limit of -10.5 dBm the MISO mode is switched to SIMO mode to give the guaranteed QoS. Above -8.99 dBm SISO gives better BER with low SNR.

After the transmitter end formulates the decision blocks, it generates a two bit EPEAS code as shown in table VI which will be sent to the receiver. Based upon the mode of the transmission chosen at the transmitter the receiver will choose its reception mode based upon the EPEAS code book.

Table VI: EPEAS code book

Transmit Power Level (dBm)	Mode of Transmission	Code
-18.502	MIMO	11
-16.502	MIMO	11
-13.500	MISO	10
-11.500	SIMO	01
-10.500	SISO	00
-8.99	SISO	00

4.2 *Transmission Phase*

The detailed flow of transmission phase of the EPEAS transceiver chain is explained with respect to the flow chart as shown in Fig 4.2.

4.2a Transmitter chain

After setting the experimental parameters as given in Table I, the preamble sequences are generated. The Short training sequence are chosen as (STS-f) = 64 samples and (STS-t) = 16 samples which is repeated 30 times giving 480 samples followed by the long training sequence (LTS) = 64 samples repeating 2.5 times giving 160 samples. Altogether we get the total preamble sequence of length 640 samples (LTS+STS). The transmitting data sequences are being generated randomly with respect to N_{OFDM} number of symbols and N_{DATA} number of data symbols.

The data bits inserted from the source are mapped using 16-QAM modulation technique and converted from serial to parallel through S-P convertor. Pilot tones are defined as, [1 1 -1 1] and the pilot sub carriers are [8 2244 58]. The pilot tones are inserted and repeated for every N_{OFDM}.

Based upon the decision block generated by EPEAS strategy as explained in section IV, the transmitter chooses the mode of transmission to be either MIMO/MISO/SIMO/SISO. If MIMO/MISO is chosen, the transmitter makes use of STBC (Alamouti scheme) as explained in section II for transmission and in the case of SIMO, it uses ECC to combine the data from both the antennas as in section II. For SISO a general OFDM link is chosen.

64-point IFFT is applied to the codeword C = [c_0 c_1.....c_{63}] generated to convert it to time domain. IDFT output at n^{th} time interval (n= 0, 1,...., 63) is given by (11), (12) and (13)

$$x_n = \frac{1}{8}\sum_{k=0}^{63} c_k e^{\frac{j2\pi kn}{64}} \quad (11)$$

In matrix form,

$$[x_0 x_1 \dots\dots x_{63}]^T = D^H [c_0 c_1 \dots\dots c_{63}]^T \quad (12)$$

$$[x_0^T x_1^T \dots\dots x_{63}^T]^T = (D^H \otimes I_2)[c_0^T c_1^T \dots\dots c_{63}^T]^T \quad (13)$$

The 64×64 matrix D^H realizes the IDFT operation. Hence D is a DFT matrix.

After converting the codeword into time domain to avoid inter-symbol interference, a guard interval vector (Cyclic Prefix) of length 16 denoted as X_g= $[x_{-16} x_{-15} \dots\dots x_1]$ is added in front of the codeword X = $[x_0 x_1 \dots\dots x_{63}]$ so that OFDM symbol X'= [X_g X].

After IFFT processing and cyclic prefix addition, parallel streams are converted into serial time domain samples using a multiplexer and making it ready for

transmission through air using multiple carrier frequencies. The data to be transmitted has to be padded with zeros in order to match the buffer size of the WARP kit. The buffer size of each radio board is 32768 bits.

The data to be transmitted is given as an input to WARP kit which will be time domain samples with real and imaginary parts. They are stored separately on I & Q buffer. The stored data is converted into analog waveforms using a DAC. Two analog waveforms are generated separately from real valued samples obtained from I & Q. Here $f_{sam}=f_{clk}$=40 MHz. The baseband signal is up-converted to RF carrier frequency. Then finally the modulated signal is amplified using RF amplifier and transmitted using Tx antenna 1 and Tx antenna 2.

4.2b Receiver Chain

At the receiver end, the mode of reception is enabled based on the EPEAS code received from the transmitter.

The RF signal is received by Rx antenna, which will be amplified using Low Noise Amplifier to increase its signal strength and then down converted into baseband frequency. The incoming signal is correlated with in phase and quadrature carrier separately to recover inphase and quadrature baseband components separately. Further the analog waveform is converted into digital samples using ADC. The sampling frequency of ADC is equal to buffer clock frequency. In phase and Quadrature samples are obtained from separate ADC's.

After conversion the samples are stored in a buffer. As the samples are not passed through the FFT block, the samples are in time domain. So received time domain LTS (Long Training Sequence) samples are correlated with received vector samples (LTS= 64 Samples).In time domain OFDM waveform involves repeated block of [LTS;STS (Short Training Sequence); Payload]. As LTS is transmitted twice while performing correlation it gives two peaks and autocorrelation gives a peak in the middle. The difference between the two peaks gives timing information about one OFDM symbol because number of samples in LTS and OFDM symbol are equal.

In a communication system, there is a difference in carrier frequency at transmitter and receiver. This offset is termed as CFO. The input carrier frequency at the receiver can vary due to Doppler Effect caused by relative motion between Tx and Rx. This is another cause of CFO. The frequency offset value is determined using equation (14),

$$r(t) = x(t)e^{j2\pi f_{\Delta} t} \quad (14)$$

Given that short preamble is periodic with $\delta_t = 0.8\ \mu s$ equation (14) is written as (15)

$$r(t-\delta t) = x(t)e^{j2\pi f_{\Delta}(t-\delta t)} \quad (15)$$

At the receiver, as both $x(t)$ and $r(t)$ are known,

Taking angle of both sides of the equation (15) we get the frequency offset as (16),

$$\Delta_f = -\frac{\forall y(t-\delta t)y^*(t)}{2\pi\delta t} \quad (16)$$

The LTS samples which are not CFO corrected are extracted. After estimating the carrier frequency offset value, each sample is rectified with respect to the offset value.

To reduce the computation complexity Zero-Forcing technique is used for estimating the channel. For a perfect CSI, the ZF detection weight matrix W is given by the pseudo-inverse of the channel matrix H, as (17)

$$W = (H^H H)^{-1} H^H \quad (17)$$

At the receiver, the guard interval is first removed and 64 output samples are gathered from the received signal which gives the expression (18)

$$[r_0^T r_1^T \dots\dots r_{63}^T]^T = H_g[x_{-16}^T x_{-15}^T \dots x_{-1}^T x_0^T \dots x_{63}^T]^T + [n_0^T n_1^T \dots\dots n_{63}^T]^T \quad (18)$$

Where H_g is 128x158 ($64n_r$ x $n_t(64+16-1)$) matrix representing the channel seen by the OFDM symbol. The system model of equation (18) is rewritten as (19),

$$[r_0^T r_1^T \dots\dots r_{63}^T]^T = H_{cp}[x_0^T \dots x_{63}^T]^T + [n_0^T n_1^T \dots\dots n_{63}^T]^T \quad (19)$$

Where H_{cp} is a block wise circulant matrix of size 128x128 matrix. As a result, its SVD decomposition $H_{cp} = (D^H \otimes I_2) D_{cp} (D \otimes I_2)$ is such that D_{cp} is a block diagonal matrix whose blocks are obtained by a block wise FFT. The full information about the channel is accounted for in D_{cp}, and the eigenvectors of H_{cp} are independent of the channel matrix H. So equation (19) is depicted as (20),

$$[r_0^T r_1^T \dots\dots r_{63}^T]^T = (D^H \otimes I_2) D_{cp} [c_0^T \dots c_{63}^T]^T + [n_0^T n_1^T \dots\dots n_{63}^T]^T \quad (20)$$

Applying a 64-FFT operation to the received vector, we finally obtain the equation as (21),

$$R = r_k = \sqrt{E_s} H_{(k)} c_k + n_k = XH + N \quad (21)$$

The ZF symbol vector estimate, $\hat{X}$ is given in (22)

$$\hat{X} = WR = (H^H H)^{-1} H^H X + (H^H H)^{-1} H^H N = X + (H^H H)^{-1} H^H N \quad (22)$$

i.e., ZF detection attempts to eliminate the inter-stream interference.

Given the estimate $\hat{H}$ of H, ZF detection estimates the symbol transmitted through the k^{th} antenna by mapping the k^{th} element of the two dimensional vector, into the closest modulation constellation symbol by using (23).

$$\widehat{W}R = \left[\hat{H}^H \hat{H}\right]^{-1} + \hat{H}^H X + \left[\hat{H}^H \hat{H}\right]^{-1} \hat{H}^H N \quad (23)$$

The Fig 4.3 shows the comparison graph of BER performance between MIMO and EPEAS. The comparison graph shows that the switched result based on EPEAS strategy excels the performance of MIMO system resulting in performance enhancement of 22.3%.

5. EPEAS POWER CALCULATION

The Fig 5.1 shows the transceiver chain of the WARP test bed. The power consumption of transmitter and receiver chain is given by the equation (24) and (25).

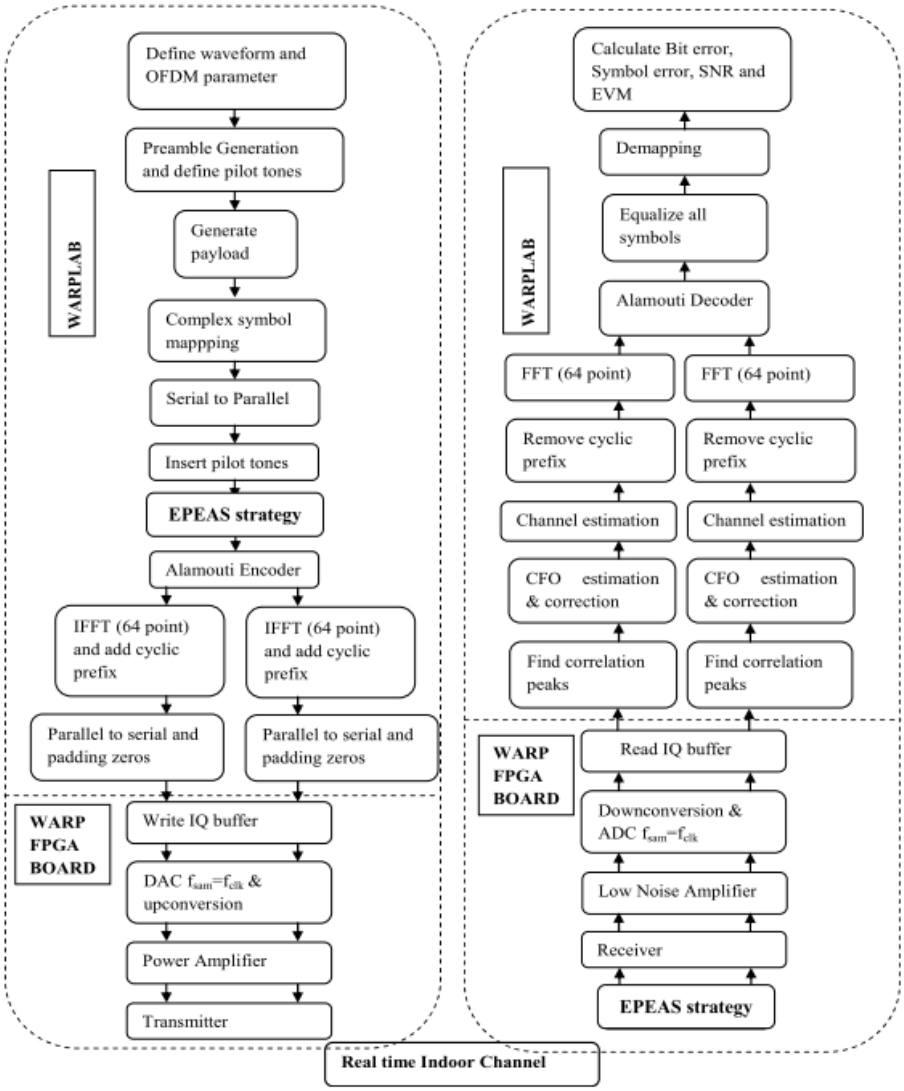

Fig. 4.2 Data Flow in EPEAS Transceiver Chain

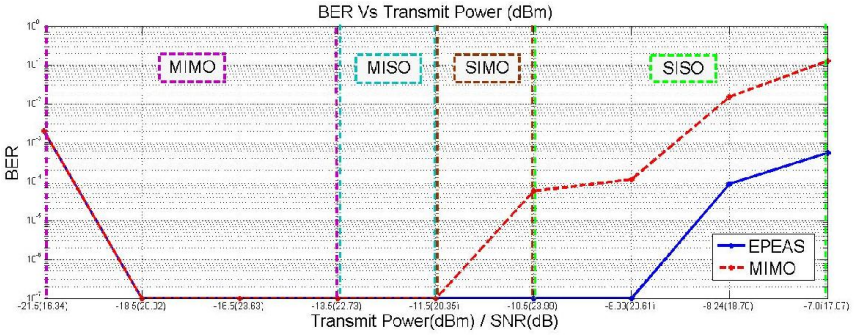

Fig. 4.3 Comparison of BER performance of EPEAS and MIMO with varying Transmit Power

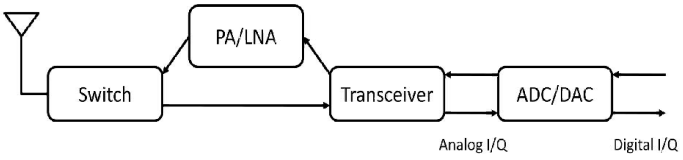

Fig 5.1 Transceiver Chain in WARP

$$P_T = P_{PA} + P_{tr} + P_{DAC} = 0.56\text{mW} + 18.19\text{mW} \quad (24)$$
$$(P_{PA} + P_{tr}) = 0.56\text{mW};\ (P_{DAC}) = 18.19\text{mW}$$
$$P_R = P_{LNA} + P_{tr} + P_{ADC} = 0.56\text{mW} + 0.14\text{mW} \quad (25)$$
$$(P_{LNA} + P_{tr}) = 0.56\text{mW};\ (P_{ADC}) = 0.14\text{mW}$$

Where, P_T and P_R are the total power consumed for transmitting and receiving the data in WARP test bed. P_{PA}, P_{LNA} and P_{tr} are the power consumed by Power Amplifier (AWL 6951), Power consumed by Low Noise Amplifier (AWL 6951) and power consumed by Transceiver IC (MAX 2829) respectively. P_{ADC} is the power consumed by ADC IC and similarly P_{DAC} are the power consumed by DAC IC.

The WARP test bed supports a data rate of 54Mbps, here we have transmitted a data of 32MB (32768 bits) which will take a time of 4 seconds to complete

one successful transmission. Table X details the power saved using EPEAS strategy. The power consumption calculation for various mode are shown below,

- For MIMO operating at -18.5dBm and -16.5dBm
  $2(P_T) + 2(P_R)$ = 2(0.014 + 18.19) + 2(0.014 + 0.14) = 36.716mW
  = 2(0.022 + 18.19) + 2(0.022 + 0.14) = 37.144mW

- MISO operating at -13.5dBm,
  $2(P_T) + P_R$=2(0.044+18.19) + (0.044+0.14) = 36.652 mW

whereas, when operated at MIMO mode at this range, 36.836mW of power is consumed.

- SIMO, operating at -11.5dBm,
  $(P_T) + 2(P_R)$ = (0.071+18.19) + 2(0.071+0.14) = 18.683mW

whereas, when operated at MIMO mode at this range, 36.943mW of power is consumed,

- SISO, operating at -10.5dBm and -8.99dBm,
  $P_T + P_R$ = (0.09+18.19) + (0.09+0.14) = 18.51mW
  = (0.12+18.19) + (0.12+0.14) = 18.57mW (37.156mW-MIMO)

Whereas, when operated at MIMO mode at this range, 36.943mW and 37.156mW of power is consumed respectively.

Table X: Power saving for various modes of Operation

Power Saved (mW) for 4 (sec)		
	Power saved	**% power saved**
MISO	0.1846	0.58%
SIMO	18.260	48.75%
SISO	18.508 & 18.586	51.22%

5. CONCLUSION

All future wireless systems (LTE, LTE-A, Wi-Max, IEEE - 802.11n, ac, e) are supported by MIMO for its evolution. The Quality of Service (QoS) of the MIMO system degrades in a highly correlated channel. Inthis paper a novel Enhanced Power Efficient Antenna Switching (EPEAS) strategy to provide a mobile user a guaranteed QoS even in a highly correlated scenario along with EVM based Constellation Combiner (ECC) is proposed. The proposed system is implemented and analyzed in real indoor channel environment using WARP test bed. It can be seen that there is a pronounced improvement of about 22.3% for the EPEAS compared to the basic MIMO technique. The future scope for this concept would be to try optimizing the decision block by using cross layer parameters.

ACKNOWLEDGEMENT

We would like to thank Department of Science and Technology, Government of India for supporting the work under the scheme of "FAST TRACK SCHEME FOR YOUNG SCIENTIST" under the grant number SR/FTP/ETA-92/2011.

REFERENCES

[1] Beyond 3G air interface technology - System level assessment of research (Phase I) report, Transmission of Information Industry Research Institute, 2004.

[2] Huawei Technologies Co., Ltd., "Improving energy efficiency, lower CO2 emission and TCO", in Energy Efficiency Solution White Paper. http://www.mobilontelecom.com/Huawei-Energy-Efficiency-White-Paper.pdf.

[3] Mohd Sufiyan Faridi, "Spatial Correlation Based MIMO mode Switching in LTE Downlink System", *IEEE International Conference on Computational Intelligence & Communication Technology*, DOI: 10.1109/CICT.2015.80, pp 438-442, 2015.

[4] Hongmei Zhang, Quanjun Zhang, Yan He, "On Correlation and SINR based MIMO Mode Switching", *8th International Conference on Communications and Networking* DOI: 10.1109/ChinaCom.2013.6694621, pp 358-362, August, 2013.

[5] Pasquale PACE, "Green Antenna Switching to improve energy saving in LTE networks", *IEEE Online Conference on Green Communications (GreenCom)*, DOI : 10.1109/GreenCom.2012.6519622, pp 92-97, September, 2012.

[6] Himal A. Suraweera, Diomidis S. Michalopoulos, George K. Karagiannidis, "Performance of Distributed Diversity Systems With a Single Amplify-and-Forward Relay", *IEEE transactions on vehicular technology*, vol. 58, no. 5, pp 2603 - 2608, June 2009.

[7] SalamaS. Ikki and MohamedH. Ahmed, "Performance of Cooperative Diversity Using Equal Gain Combining(EGC) over Nakagami-m Fading Channels", *IEEE transactions on wireless communications*, vol. 8, no. 2, pp 557 - 562, February 2009.

[8] Soumendra Nath Datta, "Performance Analysis of Distributed MRC Combining with a Single Amplify-and-Forward Relay over Rayleigh Fading Channels", *IEEE Wireless Communications and Networking Conference (WCNC)*, DOI : 10.1109/WCNC.2013.6554936, pp 2399 - 2404, April 2013.

[9] Rishad Ahmed Shafik, Md. Shahriar Rahman, AHM Razibul Islam and Nabil Shovon Ashraf. "The Error Vector Magnitude as a performance metric and comparative analysis", IEEE-ICET, *2nd International Conference on Emerging Technologies,* DOI: 10.1109/ICET.2006.335992pp 13-14, November 2006.

[10] www.warpproject.org.

[11] Mugelan R.K, Thilaga.P, Bhagyaveni M.A, "EVM based Performance Analysis of LTE Downlink & it's Real time Evaluation using WARP", *International Journal of Applied Engineering and Research*, Volume:10, Issue:2, pp 2401-2418, January 2015.

[12] Mugelan R.K, Syed Moinuddin Bokhari, Bhagyaveni M.A, "EVM based constellation combiner (ECC) for co-operative relay network", *IEEE Communication Letters*, Vol. 20, pp 304-307, February 2016.

[13] Data sheet- MAX2828/MAX2829 Single/Dual-Band 802.11a/b/g World-Band Transceiver ICs Pages 1-39, 2014.